Research Square

Preprints are preliminary reports that have not undergone peer review.
They should not be considered conclusive, used to inform clinical practice,
or referenced by the media as validated information.

Oleandrin Induces Immunogenic Cell Death Via the PERK/eIF2α/ATF4/CHOP Pathway in Breast Cancer

Xiaoxi Li
Cancer Hospital of China Medical University: Liaoning Cancer Institute and Hospital
Jian Zheng
Cancer Hospital of China Medical University: Liaoning Cancer Institute and Hospital
Shi Chen
Cancer Hospital of China Medical University: Liaoning Cancer Institute and Hospital
Fan-dong Meng
The First Affiliated Hospital of China Medical University
Jing Ning
Cancer Hospital of China Medical University: Liaoning Cancer Institute and Hospital
Shu-lan Sun (sunshulan@cancerhosp-ln-cmu.com)
Cancer Hospital of China Medical University: Liaoning Cancer Institute and Hospital
https://orcid.org/0000-0002-7624-1797

Research

Keywords: oleandrin, immunogenic cell death (ICD), endoplasmic reticulum (ER) stress, anti-tumor immune activation

Posted Date: December 29th, 2020

DOI: https://doi.org/10.21203/rs.3.rs-135608/v1

License: This work is licensed under a Creative Commons Attribution 4.0 International License.
Read Full License

Abstract

Background Chemotherapeutic agents have been linked to immunogenic cell death (ICD) induction that is capable of augmenting antitumor immune surveillance. The cardiac glycoside oleandrin, which inhibits Na^+/K^+-ATPase pump (NKP), has been shown to suppress breast cancer growth via inducing apoptosis. However, the implications of oleandrin in antitumor immune response and potential ICD induction remain unexplored till now, which is investigated in the present study.

Methods Calreticulin **(**CRT) exposure was detected by immunofluorescence and flow cytometry, and high mobility group protein B1 (HMGB1) and Adenosine Triphosphate (ATP) secretion was quantified by ELISA and both the intracellular and extracellular expression of Heat shock protein 70/90 (HSP70/90) was detected by western blotting in breast cancer cells treated with oleandrin. Dendritic cells (DCs) were co-cultured with oleandrin-treated breast cancer cells before the expressions of activation markers and cytokines were examined by quantitative real time polymerase chain reaction (qRT-PCR), ELISA, and flow cytometry. Immune activation effects of oleandrin were determined in murine breast cancer model using BALB/C mice. The differential mRNA expression incurred by oleandrin was investigated by mRNA sequencing and subsequently confirmed by qRT-PCR and Western blotting.

Results Oleandrin treatment induced CRT exposure on cell surface and the release of HMGB1, HSP70/90 and ATP. The maturation and activation of DCs were increased by co-culturing with oleandrin-treated cancer cells, which subsequently enhanced $CD8^+$ T cell cytotoxicity. In animal models, oleandrin inhibited tumor growth and increased tumor infiltrating lymphocytes including DCs and T cells. Mechanistically, oleandrin induced endoplasmic reticulum (ER) stress associated caspase independent immunogenic cell death (ICD) mainly through PERK/eIF2α/ATF4/CHOP pathway. Activation of IRE1 pathway but not ATF6, the other two canonical sensors of ER stress, was also observed.

Conclusion Oleandrin triggered ER stress and induced ICD-mediated immune destruction of breast cancer cells. Oleandrin combined with immune checkpoint inhibitors might improve the efficacy of immunotherapy.

Background

Breast cancer is the most common malignant tumor occurring in women. With the incidence and mortality rate of breast cancer increasing annually, this malignancy has remained as one of the most serious threats to women's health. In 2019, over 2 million cases of breast cancer were reported worldwide, and more than half a million patient death was attributed to breast cancer (1). Treatment options of breast cancer include surgery, radiotherapy, chemotherapy, endocrine therapy, and targeted therapy (2). However, treatment outcome is still far from satisfactory, especially for triple-negative breast cancers that lack effective treatment targets.

In recent years, immunotherapies represented by immune checkpoint inhibitors have made remarkable achievements in tumor treatment. Phase III clinical trial has showed that paclitaxel combined with

atezolizumab, a programmed death-ligand 1 (PD-L1) blocking antibody, has significantly prolonged the progression free survival and total survival of participants with metastatic triple-negative breast cancer compared with paclitaxel combined with placebo group (3). The application of atezolizumab has been approved for the treatment of advanced breast cancer. Several studies have also shown that the number and co-stimulation of tumor infiltrating lymphocytes, especially $CD4^+$ T, $CD8^+$ T cells and dendritic cells (DCs), are indicators of curative effects (4). Therefore, immune regulation holds great potential in the treatment of breast cancer and enhancement of tumor lymphocytes infiltration will likely show beneficial effects.

The immune system functions routinely to eliminate dead cells during normal cell turnover, infections and injures (5). Certain chemotherapeutic agents such as anthracyclines, oxaliplatin and paclitaxel can trigger tumor cell death via enhance immune destruction via eliciting the release of damage-associated molecular patterns (DAMPs) to enhance tumor immunogenicity. Immunogenic cell death (ICD) is a cell death process characterized by the upregulation of various DAMPs (6). Calreticulin (CRT), high mobility group box 1 (HMGB1), adenosine triphosphate (ATP) and heat shock protein 70/90 (HSP 70/90) belong to DAMPs. As an "eat me" signal, CRT attracts antigen-presenting cells (APCs) to phagocytize the dead cells. ATP acts as a "find me" signal, which leads to immune cell infiltration into tumor sites (7–10).

Na^+/K^+-ATPase pump (NKP) is a transmembrane ion transporter expressed in various cells such as neurons and cardiomyocytes (11). NKP serves as a multifunctional signal transducer that is essential for regulating cell apoptosis, inflammation, adhesion and maintaining cell homeostasis (12). NKP consists of α, β and γ subunits. The α1 and α3 subunits of NKP are frequently overexpressed in various cancers, such as colorectal cancer, glioblastoma, and breast cancer (13, 14). Interestingly, cardiac glycosides, such as NKP inhibitors that are used for many years in the treatment of cardiac congestion, were recently showed to have potentials in the treatment of cancer (15). Digoxin, a cardiac glycoside, has been reported to trigger ICD in osteosarcoma cells (16). Retrospective analysis also revealed that digoxin combined with standard chemotherapy prolonged the overall survival of patients with breast cancer, colon cancer, head and neck cancer and hepatocellular carcinoma (17).

In the present study, we report that oleandrin, a monomer compound extracted from the leaves of *Nerium oleander* that belongs to the cardiac glycoside family (18–20), suppresses breast cancer cell growth by inducing ICD and leading to increased immune destruction of tumor cells. The effects of oleandrin were linked to ER stress mainly through PERK/eIF2α/ATF4/CHOP pathway. Activation of IRE1 pathway but not ATF6, the other two canonical sensors of ER stress, was also observed. Our findings reveal the potential of oleandrin in cancer treatment via regulating antitumor immune activation.

Methods

Antibodies and reagents

Oleandrin was purchased from MedChemExpress (Monmouth Junction, NJ, USA). Anti- HSP70 (#4876), anti-ATF3 (#33593) and anti-β-actin (#3700) antibodies were purchased from Cell Signaling Technology, Inc. (Danvers, MA, USA). Anti-PERK (ab79483), anti-eIF2α (ab5369), anti-eIF2α (phosphor S52) (ab227593), anti-ATF4 (ab23760), anti-CHOP (ab11419), goat anti-mouse IgG-horseradish peroxidase (HRP) (ab205719), goat anti-Rabbit IgG-HRP (ab6721), anti-PERK (phospho T982) (ab192591), anti-IRE1 (ab37073), anti-IRE1 (phosphor S724) (ab124945), anti-XBP1 (ab37152), anti-Calreticulin (ab2907), Goat anti-rabbit IgG (Alexa Fluor®488) (ab150077) and anti-GADD34 (ab9869) antibodies were purchased from Abcam (Cambridge, MA, USA). Anti-HSP90 antibody was purchased from Santa Cruz Biotechnology, INC (Dallas, Texas, USA). PerCP anti-human HLA-DR (307627), APC anti-human CD11c (301614), FITC anti-human CD80 (305406), PE anti-human CD86 (305406) antibodies were obtained from Biolegend (San Diego, CA, USA).

Cell lines

Human breast cancer cell lines MDA-MB-231, MCF7 and T47D were obtained from the Cell Bank of the Chinese Academy of Sciences (Shanghai, China). MDA-MB-231 cells were cultured in L-15 medium. MCF7 cells were cultured in minimum Eagle's medium. T47D cells were cultured in RPMI-1640 medium. Cell culture medium was obtained from Hyclone (GE Healthcare Life Sciences, Logan, UT, USA). Mouse breast cancer cell lines EMT6 were obtained from ATCC and cultured in Waymouth's MB 752/1 medium (Biological Industries, Kibbutz Beit-Haemek, Israel). All the medium was supplemented with 10% fetal bovine serum (FBS, Gibco, Thermo Fisher Scientific, Inc.,Waltham, MA, USA).

DC culture and $CD8^+$ T cell isolation

This study was approved by the ethics committee of the Cancer Hospital of China Medical University (Ethics Review Approval no. 20170226). Two female volunteers, aged 27 and 35, were recruited and provide the informed consents. Peripheral blood was stained with HLA-A2 and HLA subtype was detected by flow cytometry. Peripheral blood mononuclear cells (PBMCs) were isolated from HLA-A2 type volunteer and cultured in 75 cm^2 flask for 1 h. Suspended cell were removed, and the adherent cells were cultured with fresh x-vivo 15 medium (Lonza, Alpharetta, GA, USA) containing 5% plasma supplemented with 500 U/ml of IL-4 and 1,000 U/ml of GM-CSF (Promega, Madison, WI, USA). After 5 days of culture, DCs were collected for following experiments. $CD8^+$ T cells were isolated from PBMCs using the $CD8^+$ T Cell Isolation Kit according to manufacturer's instructions (Miltenyi Biotec, CA, USA).

Immunofluorescence staining for CRT

Breast cancer cells were treated with oleandrin. The concentrations of oleandrin used against MCF7 and MDA-MB-231 cells were 15 nM and 25 nM, respectively. After 24 h of treatment, cells were fixed with 95% ethanol, permeabilized with PBS containing 1% Triton X-100, and blocked using 1% BSA. Cells were incubated with anti-CRT antibody (monoclonal rabbit; 1:75) at 4 °C overnight. Cells were washed 3 times with PBS and incubated with secondary antibody (goat anti-rabbit Alexa Fluor 488, 1:200) for 30 min.

Nucleus was stained with 10 μg/ml of Hoechst 33342. Samples were finally observed under a fluorescent microscope (CQ1, Yokogawa, Japan).

In vitro cytotoxicity assay

2×10^4 of MDA-MB-231 cells were seeded in 6-well plate and divided into the following 5 groups: cells co-cultured with DCs, cells co-cultured with $CD8^+$ T cells, cells pretreated with oleandrin, pretreated cells and co-cultured with DCs, pretreated cells co-cultured with DCs and $CD8^+$ T cells. MDA-MB-231 cells alone were used as control group. After 48 h of co-culture, cells were washed twice with PBS to remove the immune cells and oleandrin. Cells were continued to grow for 14 days. Finally, cells were fixed and stained with crystal violet for 15 min. The numbers of colonies were counted.

Enzyme-linked immunosorbent assays (ELISA)

Breast cancer cells were treated with oleandrin. The concentrations of oleandrin used against MCF7 and MDA-MB-231 cells were 15 nM and 25 nM, respectively. Culture supernatant was collected and secreted ATP (Promega, Madison, WI, USA) and HMGB1 (Signalway Antibody, Maryland, USA) were detected with ELISA kits according to the manufacturer's instructions. MDA-MB-231 cells pretreated with oleandrin or DMSO were co-cultured with DCs for 48 h. IL-2, IL-10 and IFN-γ from the culture supernatant were quantified using Human IL-2 Quantikine ELISA Kit (D2050), Human IL-10 Quantikine ELISA Kit (D1000B) and Human IFN-γ Quantikine ELISA Kit (DIF50C) according to the instructions.

Mouse model

Animal studies were conducted according to the experimental animal guidelines of the China Medical University animal center. 2×10^5 of EMT6 were inoculated into mammary fat pads of BALB/c mice. After 7 days, both long and short diameters of the tumors reached about 5 mm. The mice were randomly divided into 3 groups with 5 mice in each group: PBS as control group, oleandrin treatment with 0.3 mg/kg and 0.6 mg/kg groups. Oleandrin was administered intraperitoneally every day. Tumor volume was measured every day and quantified as 0.5 × length × width × width. After 7-day administration, mice were sacrificed, and tumors were weighed. Tumor primary cells and splenocytes were harvested for flow cytometric analysis.

Flow cytometric analysis

$1x10^6$ of cells were collected and suspended in 100 μl of PBS. Cells were incubated with the following antibodies 5 μl /test of each at room temperature for 30 min, PerCP anti-human HLA-DR, APC anti-human CD11c, FITC anti-human CD80, PE anti-human CD86.

Mouse primary tumor cells were minced and disassociated with the EZ enzyme (Nitta Gelatin Inc., Osaka, Japan). Single cell suspensions from mouse spleen and tumor sites were incubated with TruStain FcX™ (anti-mouse CD16/32) antibody to block non-specific staining and then stained on ice for 30 min with the

following combination: CD3-FITC/CD4-PE/CD8-APC, CD45-PerCP/CD11b-FITC/CD11c-APC. Samples were detected by BD AccuriC6 (BD Biosciences, San Jose, CA).

Western blotting

Cells were collected and lysed using radio immunoprecipitation assay (RIPA) buffer. Cell culture supernant was were centrifuged for 30 min with 10,000 xg and protein concentration was measured using the protein concentration kit (2772T, Thermo scientific, Shanghai, China). Protein was separated by 10% sodium dodecyl sulfate polyacrylamide gel electrophoresis (SDS-PAGE) and transferred to PVDF membrane. Primary antibodies were diluted and incubated at 4°C overnight. The membranes were then washed and incubated with secondary antibodies at room temperature for 1 h. Chemiluminescence was performed using Supersignal West Pico plus (Thermo Fisher Scientific, Inc.) and detected by BIO-RAD GelDoc XR+ system (Bio-Rad, Berkeley, CA, USA). Data was analyzed by Image Lab (version 5.2.1).

RNA sequencing

MCF7, MDA-MB-231 and T47D cells were treated with oleandrin for 10 h. The concentrations of oleandrin used against MCF7, MDA-MB-231 and T47D cells were 15 nM, 25 nM and 12.5 nM, respectively. Total RNA of treated cells and controls were extracted using TRIzol. The mRNA was sequenced using the Illumina Hiseq platform. Differential expression analysis of two groups was performed using the DESeq2 R package (1.16.1). The data were transformed into Venn's diagrams and heat-map. Gene Ontology (GO) and KEGG enrichment analysis of differentially expressed genes was implemented by the cluster Profiler R package.

Quantitative real time polymerase chain reaction (qRT-PCR)

Cells were lysed with 1 mL of TRIzol reagent (Thermo Fisher Scientific, Carlsbad, CA, USA), and cDNA was synthesized with the PrimeScript™RT reagent Kit (TaKaRa, Shiga, Japan). qRT-PCR was performed by using SYBR Premix EXtaq (TaKaRa, Shiga, Japan). Primers used are as follow:

CD86: forward, 5'-CTGCTCATCTATACACGGTTACC-3'

reverse, 5'-GGAAACGTCGTACAGTTCTGTG-3'

CD80: forward, 5'-GGCCCGAGTACAAGAACCG-3'

reverse, 5'-TCGTATGTGCCCTCGTCAGAT-3'

IL-2: forward, 5'- TCCTGTCTTGCATTGCACTAAG-3'

reverse, 5'- CATCCTGGTGAGTTTGGGATTC-3'

IL-10: forward, 5'-TCAAGGCGCATGTGAACTCC-3'

reverse, 5'-GATGTCAAACTCACTCATGGCT-3'

IFN-γ: forward, 5’-TCGGTAACTGACTTGAATGTCCA-3’

reverse, 5’- TCGCTTCCCTGTTTTAGCTGC-3’

GAPDH: forward, 5’-ACAACTTTGGTATCGTGGAAGG-3’

reverse, 5’- GCCATCACGCCACAGTTTC-3’

Statistical analysis

Statistical analysis was performed using the Statistical Package for the Social Sciences (SPSS) software version 21 (IBM Corp., Armonk, NY, USA). The results were represented as mean ± standard deviation. The comparison between the two groups was conducted by t-test or one-way ANOVA. $p<0.05$ was considered statistically significant (*, $p<0.05$, **, $p<0.01$).

Results

Oleandrin induces ICD in breast cancer cells *in vitro*

Our previous study has established the IC50 concentrations of oleandrin against MCF7 and MDA-MB-231 cells, which were 14.5 nM and 24.62 nM, respectively (21). Therefore, the treatment concentrations of MCF7 and MDA-MB-231 cells were used at 15 nM and 25 nM in the following experiments. CRT exposure on cell surface, a marker for ICD, is an 'eat me' signal to stimulate DC maturation and immune activation. To investigate whether oleandrin induces ICD in breast cancer, MCF7 and MDA-MB-231 cells were treated with oleandrin for 10 h before immunofluorescence assays to stain CRT (Fig. 1A). Compare to the control, oleandrin treatment increased CRT expression on cell surface. Which was further confirmed by flow cytometry analyses. The proportion of PI^-/CRT^+ subpopulation was compared between the control and oleandrin treatment group (Fig. 1B). Consistent with immunofluorescence results, oleandrin treatment increased cell surface CRT expression in both MCF7 and MDA-MB-231 cells. The release of other DAMPs, including HMGB1, ATP and HSP70/90, was also compared between the control and oleandrin-treated groups. The secreted HMGB1 was detected after 12 h and increased significantly at 24 h and 48 h in MCF7 cells following oleandrin treatment. No significant release of HMGB1 was observed in MDA-MB-231 cells at 12 h but increased significantly at 24 h and 48 h (Fig. 2A). Distinct from the results of HMGB1 release, ATP secretion was observed 4 h after oleandrin treatment in both MCF7 and MDA-MB-231 cells and reached the peaks at 12 h (Fig. 2B). Moreover, both the intracellular and extracellular expressions of HSP70/90 were detected, as presented in Fig. 2C, intracellular expressions of HSP70/90 were not affected by oleandrin in MCF7 and MDA-MB-231 cells. However, the extracellular expression of HSP70 and HSP90 were detected in both cells at 48 h after oleandrin treatment. These data indicated that oleandrin treatment triggered ICD in breast cancer cells.

Oleandrin induces ICD-associated immune activation *in vitro*

Tumor cell ICD is capable of inducing antigen presenting function of DCs. As a result, a series of immune responses are activated, including cytokine secretion and T cell activation (22). To eliminate the uncertainty caused by different human leukocyte antigen (HLA), we detected the HLA subtypes of MCF7, MDA-MB-231 cells and two volunteers. As shown in supplementary Fig. 1A and B, HLA subtype of MDA-MB-231 was HLA-A2 that matched that of the volunteer. To investigate whether oleandrin treatment induces DC maturation and activation, we cultured DCs isolated from PBMC and then co-cultured with MDA-MB-231 cells with or without oleandrin treatment. The morphologic features of DCs were observed, which showed that the adherent cells were round or oval on day 1 and extended branched projections on day 5 (sFig. 1C). Flow cytometry data confirmed that 99.37±0.15 % of cells were CD11c positive that indicated mature DCs on day 5 (Fig. 3B). DCs were co-cultured with MDA-MB-231 cells at a ratio of 1:1 with or without oleandrin treatment. After 48 h of co-culture, DCs were stained with CD45 and separated by a cell sorter (sFig. 1E). DC maturation and activation markers (CD80, CD86 and cytokine expression in DCs) were detected by qRT-PCR. The expression levels of CD80, CD86, IL-10, IL-2 and IFN-γ genes were not affected by oleandrin alone. However, co-culture of DCs with MDA-MB-231 cells increased the expression of IL-10, IL-2 and IFN-γ, but had no effects on CD80 and CD86 expressions. Compared with DC/MDA-MB-231 group, DCs co-cultured with oleandrin-treated MDA-MB-231 cells showed significantly enhanced levels of CD80, CD86, IL-2 and IFN – γ but decreased IL-10 expression. The effects on IL-2 and IL-10 were dose-dependent on oleandrin (Fig. 3A, ***p<0.01*). The expressions of PD-L1 and Tim-3 on DCs were not changed by oleandrin treatment (data not shown).

Cell surface expressions of CD80, CD86, and HLA-DR were detected by flow cytometry and represented by Δ mean fluorescence intensity (ΔMFI). Cells stained with isotype control were considered as control (Fig. 3B). IL-2, IL-10, and IFN-γ expressions in the co-culture supernatant were further confirmed by ELISA (Fig. 3C). Consistent with the qRT-PCR results, DCs co-cultured with oleandrin-treated MDA-MB-231 cells showed significantly enhanced levels of CD86, IL-2 and IFN-γ but decreased IL-10 expression. Taken together, these results suggest that co-culture with oleandrin-treated breast cancer cells significantly enhanced DC maturation and activation.

DCs, as antigen-presenting cells, cross-present tumor-associated antigens to cytotoxic $CD8^+$ T lymphocytes (23). To investigate whether oleandrin treatment enhances DC-mediated anti-tumor response, MDA-MB-231 cells treated with oleandrin were co-cultured with DCs and $CD8^+$ T cells, and cell growth were detected by colony formation assay. Cell experiment groups were divided as follows: MDA-MB-231/DCs, MDA-MB-231/$CD8^+$ T cells, pretreated MDA-MB-231, MDA-MB-231/DCs/$CD8^+$ T cells, pretreated MDA-MB-231/DCs/ $CD8^+$ T cell and cell growth was 89.8±2.14 %, 45.24±1.19 %, 51.11±2.60 %, 19.97±3.12 %, 0.01±0.0017 %, respectively (Fig. 3D). Therefore, pretreated with oleandrin enhanced DCs mediated T cell cytotoxicity *in vitro*.

Oleandrin suppresses tumor growth in mouse model

To investigate the anti-tumor effects of oleandrin *in vivo*, BALB/c mice were used to implant EMT-6 cells into mammary fat pads. 7 days after implantation, tumor-bearing mice were divided into three groups

and treated with oleandrin at 0.3 mg/kg and 0. 6mg/kg in peritoneal. Mice treated with vehicle were used as control (Fig. 4A). Compared with the control group, tumor growth was inhibited in the oleandrin treatment groups 1 day after administration. After 7 days of continuous administration, the average tumor size of 0.3 mg/kg treatment group was unchanged compared with day 0, while the average tumor size of 0.6 mg/kg treatment group was even smaller than that at day 0 (Fig. 4B, *$p<0.05$, **$p<0.01$). The average tumor weight of 0.6 mg/kg treatment group was 1.58 times lower than that of 0.3 mg/kg treatment group and was 2.66 times lower than that of the control group (Fig. 4 C and D, **$p<0.01$).

Oleandrin activates antitumor immune responses in mice

To investigate the alterations in the immune microenvironment after oleandrin treatment, splenocytes and tumor primary cells were collected and stained with T cell and DC markers. As presented in Fig. 5A-D, compared with the control group, oleandrin treatment groups showed increased populations of both $CD4^+$ and $CD8^+$ T cell in spleen in a dose-dependent manner (Fig. 5A and B, **$p<0.01$). $CD11b^+/CD11c^+$ or $CD11b^+/CD11c^-$ cells were not changed (Fig. 5C and D).

Furthermore, tumor infiltrating lymphocytes (TILs) were analyzed by staining with CD45. Compared with the control group, oleandrin treatment increased the portion of $CD45^+$ cells in a dose-dependent manner (Fig. 5E). Moreover, DC ($CD45^+/CD11c^+$) were also increased by oleandrin treatment (Fig. 5E and F, **$p<0.01$). Compared with $CD45^+$ cells and $CD11c^+$ cells, the proportion of tumor infiltrating T cells were much less. Therefore, the absolute numbers of $CD4^+$ and $CD8^+$ T cells were analyzed. As shown in Fig. 5G and H, oleandrin treatment increased the numbers of both $CD4^+$ and $CD8^+$ T cells (**$p<0.01$). These data indicated that oleandrin treatment increased DC and T cell infiltration in the tumor sites.

Oleandrin-induced CRT exposure is independent of caspase activity.

Translocation of CRT from endoplasmic reticulum (ER) to cell surface is an indicator for ICD. Previous studies have revealed that chemotherapeutic agents such as anthracyclines and oxaliplatin can induce ICD in tumor cells via caspase-8 dependent pathway. Caspase-8 hydrolyzes the ER anchor protein B cell receptor-associated protein 31 (BAP31), which further transfers CRT to cell surface through Golgi apparatus (24, 25). This procedure is essential, as blocking caspase 8 inhibits CRT exposure. Our previous study has shown that oleandrin induced breast cancer cell apoptosis. To explore whether oleandrin-induced ICD is dependent on caspase, MCF7 and MDA-MB-231 cells were pretreated with Z-VAD-FMK, a pan-caspase inhibitor, for 10 h before treated with oleandrin. Cell apoptosis and CRT exposure were detected by flow cytometry. As shown in Fig. 6A, Z-VAD-FMK significantly inhibited breast cancer cell apoptosis. However, CRT exposure was not affected (Fig. 6B). These data indicated that oleandrin-induced CRT exposure was likely not associated with caspase.

Oleandrin induces ICD via ER stress

To further explore the mechanism of oleandrin-induced ICD in breast cancer cells, MCF7, T47D and MDA-MB-231 cells were treated with oleandrin and differential mRNA expressions were analyzed by RNA

sequencing. A total of 121 common significantly different genes in the three different pairs of cells were identified in the Venn's diagrams (Fig.7A). The most significantly changed genes were categorized into the ATF2 pathway (Fig.7B). The identified genes involved in ATF2 pathway were illustrated using a heat-map. As shown in Fig.7C, activating transcription factor 3 (*ATF3*), DNA damage inducible transcript 3 (*DDIT3*), and activating transcription factor 4 (*ATF4*) were reported as the downstream genes of the ER stress pathway. Their altered expressions were further validated by qRT-PCR (Fig. 7D). The mRNA expression levels of these three genes were confrmed to be up-regulated by oleandrin treatment. Consistent with qRT-PCR results, the protein expression levels of ATF3, ATF4 and CHOP (*DDIT3*) were also increased accordingly (Fig. 7D). These data indicated that oleandrin-induced ICD might be associated with ER stress.

Oleandrin induces ER stress in breast cancer

In mammalian cells, various cytotoxic stimuli can cause unfolded protein responses (UPRs), which function as an adaptive cellular program to sustain protein homeostasis to protect cells (26). Such imbalance incurred by various stimuli can cause ER stress. ER stress is initiated by three ER transmembrane sensors: protein kinase R–like ER kinase (PERK), inositol requiring enzyme 1α (IRE1) and activating transcription factor 6 (ATF6). Three sensors can further activate downstream signaling pathways. The expression of total PERK, its substrate eukaryotic translation initiation factor 2α (eIF2α) and ATF6 were not affected by oleandrin treatment (Fig. 8A and sFig. 1F). However, phosphorylation levels of PERK and eIF2α (S52) were enhanced 6 h after oleandrin treatment. In addition, the activation of ATF4, and the expressions of ATF4-dependent target protein (growth-arrest- and DNA-damage-induced transcript 34 (GADD34, PPP1R15A) and CHOP) were increased as well (Fig.8A). Previous studies have demonstrated that GADD34 associates with the broadly acting serine/threonine protein phosphatase 1 (PP1) to dephosphorylate eIF2α (27). This may be a feedback mechanism for cell homeostasis. Moreover, the expression of IRE1 and phosphorylation of IRE1 (S724) were significantly increased, and subsequently enhanced the downstream XBP1 expression (Fig. 8B).

As shown in Fig. 9, oleandrin, as a Na^+/K^+ ATPase inhibitor, increases the concentration of Na^+ and activated Na^+/Ca^{2+} ion exchange channel on cell surface, which causes the influx of Ca^{2+}. Loss of cellular homeostasis and disruption of Ca^{2+} leads to activation of ER stress associated pathways including PERK-eIF2α-ATF4 and IRE1-XBP1. ER stress enhances the releasement of ATP and HMGB1. Moreover, ER stress induces CRT exposure to the cell surface. The release of these DAMPs signals eventually leads to the enhancement of immune response.

Discussion

Nerium oleander is widely distributed in subtropical Asia, Mediterranean coast and southwest America. The flowers and leaves are commonly used in folk medicine for the treatment of heart failure, leprosy, analgesic, malaria, ringworms, anti-inflammatory and indigestion.(28, 29). Oleandrin is a monomer compound extracted from the leaves of *Nerium oleander* contains potent cardenolides which shows

strong heart clinical effect (30, 31). Recent studies have revealed that oleandrin has antitumor activities in various tumors such as ovarian cancer, glioma, colon cancer, osteosarcoma, bladder cancer, breast cancer and leukemia. The working mechanism involves the suppression of Akt phosphorylation and the inhibition of mTOR (32–36). The botanical drug candidates of oleandrin, Anvirzel™ and PBI-05204, have been tested in phase I clinical trials for the treatment of solid tumors. Pbi-05204 was administered under a dose of 0.2255 mg/kg/day, and no side effects above grade 3 occurred, which proved its safety in patients with advanced cancer (37). Our previous study demonstrated that oleandrin had obvious cytotoxic effects on MCF7 (Luminal A subtype), SK-BR-3 ($HER2^+$ subtype) and MDA-MB-231 (TNBC subtype) cells, but no obvious inhibitory effect on MCF10a was observed (21).

DCs are potent antigen presenting cells and play an important role in ICD-mediated immune response. In this study, we show that DC maturation and activation were not affected by oleandrin treatment. However, CD80 expression increased significantly on DCs co-cultured with oleandrin-pretreated MDA-MB-231 cells. CD80 along with CD86 that are markers of active DCs bind to CD28 on T cells and act as a costimulatory signal for T cell activation (38). Moreover, oleandrin treatment decreased IL-10 expression but increased IL-2 and IFN-γ secretion. As an immunosuppressive cytokine, IL-10 inhibits the function of DC cells and weakens the immune activities of $CD4^+$ and $CD8^+$ T cells (39). IL-2 plays an essential role for the proliferation of antigen specific T cells (40). IFN-γ induces the differentiation of Th1 and NKT cells and is important for anti-tumor immunity (41). These data indicate that oleandrin triggered ICD and activated DC-mediated immune responses. Consistent with our hypothesis, cytotoxic activities of $CD8^+$ T cells were enhanced by oleandrin pretreatment *in vitro*. *In vivo* experiments further confirmed that intraperitoneal administration of oleandrin at both 0.3 mg/kg and 0.6 mg/kg inhibited tumor growth. Oleandrin treatment increased the number of tumor infiltrating $CD45^+$ cells including $CD11c^+$ DCs, $CD4^+$ T cells and $CD8^+$ T cells. The infiltrations of $CD4^+$ and $CD8^+$ T cells were dose dependent, especially in $CD8^+$ T cells. Furthermore, we analyzed T cells in tumor-bearing mice using splenocyte preparations and found that oleandrin increased the portion of both $CD4^+$ and $CD8^+$ T cells in the spleen. These data suggested oleandrin treatment induced ICD and stimulated DC-mediated immune responses *in vivo*.

ICD activates anti-tumor immune response mainly by releasing DAMPs. CRT exposure, ATP secretion and HMGB1 release are all indispensable for ICD, meaning that the absence of one single of these ICD hallmarks abolishes its efficacy (6). In the present study, CRT exposure was observed in MCF7 and MDA-MB-231 breast cancer cells 6 hours after oleandrin treatment. Consistent with the previous study, CRT exposure is earlier than cell apoptosis, which indicates CRT exposure was not the consequent event of DNA damage (9). Endoplasmic reticulum, where CRT locates, plays a crucial role in the maintenance of intracellular signal transduction, protein synthesis and calcium homeostasis (42). The RNA sequencing results suggested that oleandrin-induced ER-stress was associated with ICD. Previous studies have shown that certain chemotherapy agents such as anthracyclines and oxaliplatin induce ER stress via activating the caspase-8 signaling pathway that regulates CRT exposure. Caspase-8 hydrolyzes ER binding protein BAP31, which releases CRT from ER to cell surface (24, 25). However, in this study, Z-VAD-FMK, a caspase inhibitor, significantly inhibited the cell apoptosis, but had no significant effect on CRT

exposure, indicating that the CRT exposure induced by oleandrin was not dependent on caspase pathway. Western blotting results further confirmed that oleandrin treatment activated ATF3 and CHOP via PERK-eIF2α-ATF4 and IRE1-XBP1 pathways but not ATF6. ER stress culminates in the translocation of the CRT to the cell surface, thereby generating an ‘eat-me’ signal for DCs

In the present study, ATP secretion was detectable after 6 h but HMGB1 release was confirmed after 24 h following oleandrin treatment. In the early stage of ER stress, in order to maintain cell homeostasis, cells activate autophagy which facilitates the release of ATP from dying cells (43, 44). ATP, as a ‘find-me’ signal, recruits DCs to the dying cells. Distinct from ATP secretion, HMGB1 was passively released into the extracellular space at later post-apoptotic time point, allowing HMGB1 to bind Toll-like receptor 4 on DCs and thus stimulate their antigen presentation functions (45). Moreover, previous study demonstrated that CHOP regulates the release of HMGB1 (46). Therefore, we speculated CRT exposure, ATP secretion and HMGB1 release were associated with ER stress (Fig. 9).

Immunotherapies represented by immune checkpoint inhibitors have shown promising therapeutic outcomes. PD-L1 overexpression, tumor mutation burden (TMB) and tumor infiltrating lymphocytes affect the efficiency of immunosuppressive agents (47). The number and function of tumor infiltrating lymphocytes, especially $CD4^+$ T cells, $CD8^+$ T cells and DCs, are key to the effectiveness of the immunotherapy (4). Immune checkpoint inhibitors combining with ICD-inducing agents might be a more effective approach, especially in the treatment of tumors lacking immune cell invasion that are referred as “cold tumor”. Recently, it was demonstrated that immune checkpoint inhibitors increased the antitumor response while combined with ICD-inducing chemotherapy agents or radiation therapy (48, 49). Several clinical trials that combine checkpoint inhibitors with ICD inducers are ongoing, and the hope is that these combinations will increase the number of patients who can benefit from checkpoint inhibitor therapies. Further study is needed to demonstrate that whether oleandrin combined with immune checkpoint inhibitors will improve the efficacy of immunotherapy and reduce the side effects of chemotherapeutics through dose reduction.

Conclusions

Oleandrin triggered ER stress and induced ICD-mediated immune destruction of breast cancer cells. Oleandrin combined with immune checkpoint inhibitors might improve the efficacy of immunotherapy.

Abbreviations

ICD: immunogenic cell death; NKP: Na^+/K^+-ATPase pump; qRT-PCR: quantitative real time polymerase chain reaction; ER stress: endoplasmic reticulum stress; PD-L1: programmed death-ligand 1; DCs: dendritic cells; DAMPs: damage associated molecular patterns; CRT: Calreticulin; HMGB1: high mobility group box 1; ATP: Adenosine Triphosphate; APC: antigen-presenting cell; PBMC: Peripheral blood mononuclear cell; ELISA: Enzyme-linked immunosorbent assays; PD-L1: programmed death-ligand 1; HLA: human leukocyte antigen; ΔMFI: Δ mean fluorescence intensity; TILs: tumor infiltrating lymphocytes;

BAP31: B cell receptor-associated protein 31; ATF3: activating transcription factor 3; CHOP, DDIT3: DNA damage inducible transcript 3; ATF4: activating transcription factor 4; UPR: unfolded protein response; PERK: protein kinase R–like ER kinase; IRE1: inositol requiring enzyme 1α; ATF6: activating transcription factor 6; eIF2α: eukaryotic translation initiation factor 2α; GADD34, PPP1R15A: growth arrest and DNA damage-inducible transcript 34.

Declarations

Ethics approval and consent to participate

This study was approved by the ethics committee of the Cancer Hospital of China Medical University (Ethics Review Approval no. 20170226). All the participants were provided the informed consents.

Consent for publication

Not applicable

Availability of data and materials

The datasets used and/or analyzed during the current study are available from the corresponding author on reasonable request.

Competing interests

The authors declare that they have no competing interests.

Funding

This work was supported by the National Natural Science Foundation of China (No. 81702621), the Natural Science Foundation of Liaoning Province (20180550618), and Young Scientist and Technology Innovation Project of Shenyang City (RC190434) to SL. S.

Authors' contributions

Study design: Xiaoxi Li; Data Collection: Xiaoxi Li, Jian Zheng and Shi Chen; Data analysis: Fan-dong Meng, Jing Ning and Shu-lan Sun; Manuscript preparation: Shu-lan Sun. All authors read and approved the final manuscript.

Acknowledgements

Not applicable

References

1. Britt KL, Cuzick J, Phillips KA. Key steps for effective breast cancer prevention. Nature reviews Cancer. 2020;20(8):417–36.
2. Matsen CB, Neumayer LA. Breast cancer: a review for the general surgeon. JAMA surgery. 2013;148(10):971–9.
3. Schmid P, Adams S, Rugo HS, Schneeweiss A, Barrios CH, Iwata H, et al. Atezolizumab and Nab-Paclitaxel in Advanced Triple-Negative Breast Cancer. N Engl J Med. 2018;379(22):2108–21.
4. Homet Moreno B, Zaretsky JM, Garcia-Diaz A, Tsoi J, Parisi G, Robert L, et al. Response to Programmed Cell Death-1 Blockade in a Murine Melanoma Syngeneic Model Requires Costimulation, CD4, and CD8 T Cells. Cancer immunology research. 2016;4(10):845–57.
5. Ricklin D, Hajishengallis G, Yang K, Lambris JD. Complement: a key system for immune surveillance and homeostasis. Nat Immunol. 2010;11(9):785–97.
6. Kroemer G, Galluzzi L, Kepp O, Zitvogel L. Immunogenic cell death in cancer therapy. Annu Rev Immunol. 2013;31:51–72.
7. Kohles N, Nagel D, Jungst D, Stieber P, Holdenrieder S. Predictive value of immunogenic cell death biomarkers HMGB1, sRAGE, and DNase in liver cancer patients receiving transarterial chemoembolization therapy. Tumour biology: the journal of the International Society for Oncodevelopmental Biology Medicine. 2012;33(6):2401–9.
8. Martins I, Wang Y, Michaud M, Ma Y, Sukkurwala AQ, Shen S, et al. Molecular mechanisms of ATP secretion during immunogenic cell death. Cell death differentiation. 2014;21(1):79–91.
9. Obeid M, Tesniere A, Ghiringhelli F, Fimia GM, Apetoh L, Perfettini JL, et al. Calreticulin exposure dictates the immunogenicity of cancer cell death. Nature medicine. 2007;13(1):54–61.
10. Tesniere A, Panaretakis T, Kepp O, Apetoh L, Ghiringhelli F, Zitvogel L, et al. Molecular characteristics of immunogenic cancer cell death. Cell death differentiation. 2008;15(1):3–12.
11. Pressley TA. Structure and function of the Na,K pump: ten years of molecular biology. Miner Electrolyte Metab. 1996;22(5–6):264–71.
12. Ko YS, Rugira T, Jin H, Park SW, Kim HJ. Oleandrin and Its Derivative Odoroside A, Both Cardiac Glycosides, Exhibit Anticancer Effects by Inhibiting Invasion via Suppressing the STAT-3 Signaling Pathway. International journal of molecular sciences. 2018;19(11).
13. Winnicka K, Bielawski K, Bielawska A, Surazynski A. Antiproliferative activity of derivatives of ouabain, digoxin and proscillaridin A in human MCF-7 and MDA-MB-231 breast cancer cells. Biol Pharm Bull. 2008;31(6):1131–40.
14. Sakai H, Suzuki T, Maeda M, Takahashi Y, Horikawa N, Minamimura T, et al. Up-regulation of Na(+),K(+)-ATPase alpha 3-isoform and down-regulation of the alpha1-isoform in human colorectal cancer. FEBS Lett. 2004;563(1–3):151–4.
15. Cherniavsky Lev M, Karlish SJ, Garty H. Cardiac glycosides induced toxicity in human cells expressing alpha1-, alpha2-, or alpha3-isoforms of Na-K-ATPase. American journal of physiology Cell physiology. 2015;309(2):C126-35.

16. Menger L, Vacchelli E, Adjemian S, Martins I, Ma Y, Shen S, et al. Cardiac glycosides exert anticancer effects by inducing immunogenic cell death. Science translational medicine. 2012;4(143):143ra99.
17. Calderon-Montano JM, Burgos-Moron E, Orta ML, Maldonado-Navas D, Garcia-Dominguez I, Lopez-Lazaro M. Evaluating the cancer therapeutic potential of cardiac glycosides. BioMed research international. 2014;2014:794930.
18. Martelli A. Results of the use of oleandrin in therapy of myocardial insufficiency; review and personal experience. Minerva Med. 1954;45(20):690–4.
19. Patel S. Plant-derived cardiac glycosides: Role in heart ailments and cancer management. Biomed Pharmacother. 2016;84:1036–41.
20. Botelho AFM, Santos-Miranda A, Joca HC, Mattoso CRS, de Oliveira MS, Pierezan F, et al. Hydroalcoholic extract from Nerium oleander L. (Apocynaceae) elicits arrhythmogenic activity. J Ethnopharmacol. 2017;206:170–7.
21. Li XX, Wang DQ, Sui CG, Meng FD, Sun SL, Zheng J, et al. Oleandrin induces apoptosis via activating endoplasmic reticulum stress in breast cancer cells. Biomedicine & pharmacotherapy = Biomedecine & pharmacotherapie. 2020;124:109852.
22. Li W, Yang J, Luo L, Jiang M, Qin B, Yin H, et al. Targeting photodynamic and photothermal therapy to the endoplasmic reticulum enhances immunogenic cancer cell death. Nat Commun. 2019;10(1):3349.
23. Mami-Chouaib F, Blanc C, Corgnac S, Hans S, Malenica I, Granier C, et al. Resident memory T cells, critical components in tumor immunology. J Immunother Cancer. 2018;6(1):87.
24. Panaretakis T, Kepp O, Brockmeier U, Tesniere A, Bjorklund AC, Chapman DC, et al. Mechanisms of pre-apoptotic calreticulin exposure in immunogenic cell death. EMBO J. 2009;28(5):578–90.
25. Zitvogel L, Kepp O, Senovilla L, Menger L, Chaput N, Kroemer G. Immunogenic tumor cell death for optimal anticancer therapy: the calreticulin exposure pathway. Clinical cancer research: an official journal of the American Association for Cancer Research. 2010;16(12):3100–4.
26. Kim I, Xu W, Reed JC. Cell death and endoplasmic reticulum stress: disease relevance and therapeutic opportunities. Nature reviews Drug discovery. 2008;7(12):1013–30.
27. Rojas M, Vasconcelos G, Dever TE. An eIF2alpha-binding motif in protein phosphatase 1 subunit GADD34 and its viral orthologs is required to promote dephosphorylation of eIF2alpha. Proc Natl Acad Sci U S A. 2015;112(27):E3466-75.
28. Begum S, Siddiqui BS, Sultana R, Zia A, Suria A. Bio-active cardenolides from the leaves of Nerium oleander. Phytochemistry. 1999;50(3):435–8.
29. Sharma P, Choudhary AS, Parashar P, Sharma MC, Dobhal MP. Chemical constituents of plants from the genus Nerium. Chem Biodivers. 2010;7(5):1198–207.
30. Cao YL, Zhang MH, Lu YF, Li CY, Tang JS, Jiang MM. Cardenolides from the leaves of Nerium oleander. Fitoterapia. 2018;127:293–300.

31. Tian DM, Cheng HY, Jiang MM, Shen WZ, Tang JS, Yao XS. Cardiac Glycosides from the Seeds of Thevetia peruviana. J Nat Prod. 2016;79(1):38–50.
32. Garofalo S, Grimaldi A, Chece G, Porzia A, Morrone S, Mainiero F, et al. The Glycoside Oleandrin Reduces Glioma Growth with Direct and Indirect Effects on Tumor Cells. The Journal of neuroscience: the official journal of the Society for Neuroscience. 2017;37(14):3926–39.
33. Ma Y, Zhu B, Liu X, Yu H, Yong L, Liu X, et al. Inhibition of oleandrin on the proliferation show and invasion of osteosarcoma cells in vitro by suppressing Wnt/beta-catenin signaling pathway. Journal of experimental clinical cancer research: CR. 2015;34:115.
34. Pan L, Zhang Y, Zhao W, Zhou X, Wang C, Deng F. The cardiac glycoside oleandrin induces apoptosis in human colon cancer cells via the mitochondrial pathway. Cancer Chemother Pharmacol. 2017;80(1):91–100.
35. Sreenivasan Y, Raghavendra PB, Manna SK. Oleandrin-mediated expression of Fas potentiates apoptosis in tumor cells. J Clin Immunol. 2006;26(4):308–22.
36. Yong L, Ma Y, Liang C, He G, Zhao Z, Yang C, et al. Oleandrin sensitizes human osteosarcoma cells to cisplatin by preventing degradation of the copper transporter 1. Phytother Res. 2019;33(7):1837–50.
37. Hong DS, Henary H, Falchook GS, Naing A, Fu S, Moulder S, et al. First-in-human study of pbi-05204, an oleander-derived inhibitor of akt, fgf-2, nf-kappaBeta and p70s6k, in patients with advanced solid tumors. Investig New Drugs. 2014;32(6):1204–12.
38. Sansom DM, Manzotti CN, Zheng Y. What's the difference between CD80 and CD86? Trends in immunology. 2003;24(6):314–9.
39. Boks MA, Kager-Groenland JR, Haasjes MS, Zwaginga JJ, van Ham SM, ten Brinke A. IL-10-generated tolerogenic dendritic cells are optimal for functional regulatory T cell induction–a comparative study of human clinical-applicable DC. Clinical immunology. 2012;142(3):332–42.
40. Funsten JR, Murillo Brizuela KO, Swatzel HE, Ward AS, Scott TA, Eikenbusch SM, et al. PKC signaling contributes to chromatin decondensation and is required for competence to respond to IL-2 during T cell activation. Cellular immunology. 2020;347:104027.
41. Alspach E, Lussier DM, Schreiber RD. Interferon gamma and Its Important Roles in Promoting and Inhibiting Spontaneous and Therapeutic Cancer Immunity. Cold Spring Harbor perspectives in biology. 2019;11(3).
42. Bezu L, Sauvat A, Humeau J, Gomes-da-Silva LC, Iribarren K, Forveille S, et al. eIF2alpha phosphorylation is pathognomonic for immunogenic cell death. Cell Death Differ. 2018;25(8):1375–93.
43. Ogata M, Hino S, Saito A, Morikawa K, Kondo S, Kanemoto S, et al. Autophagy is activated for cell survival after endoplasmic reticulum stress. Molecular cellular biology. 2006;26(24):9220–31.
44. Cirone M, Gilardini Montani MS, Granato M, Garufi A, Faggioni A, D'Orazi G. Autophagy manipulation as a strategy for efficient anticancer therapies: possible consequences. Journal of experimental clinical cancer research: CR. 2019;38(1):262.

45. Dudek AM, Garg AD, Krysko DV, De Ruysscher D, Agostinis P. Inducers of immunogenic cancer cell death. Cytokine Growth Factor Rev. 2013;24(4):319–33.
46. Zhang M, Guo Y, Fu H, Hu S, Pan J, Wang Y, et al. Chop deficiency prevents UUO-induced renal fibrosis by attenuating fibrotic signals originated from Hmgb1/TLR4/NFkappaB/IL-1beta signaling. Cell death disease. 2015;6:e1847.
47. Gibney GT, Weiner LM, Atkins MB. Predictive biomarkers for checkpoint inhibitor-based immunotherapy. The Lancet Oncology. 2016;17(12):e542-e51.
48. Twyman-Saint Victor C, Rech AJ, Maity A, Rengan R, Pauken KE, Stelekati E, et al. Radiation and dual checkpoint blockade activate non-redundant immune mechanisms in cancer. Nature. 2015;520(7547):373–7.
49. Dovedi SJ, Adlard AL, Lipowska-Bhalla G, McKenna C, Jones S, Cheadle EJ, et al. Acquired resistance to fractionated radiotherapy can be overcome by concurrent PD-L1 blockade. Cancer Res. 2014;74(19):5458–68.

Figures

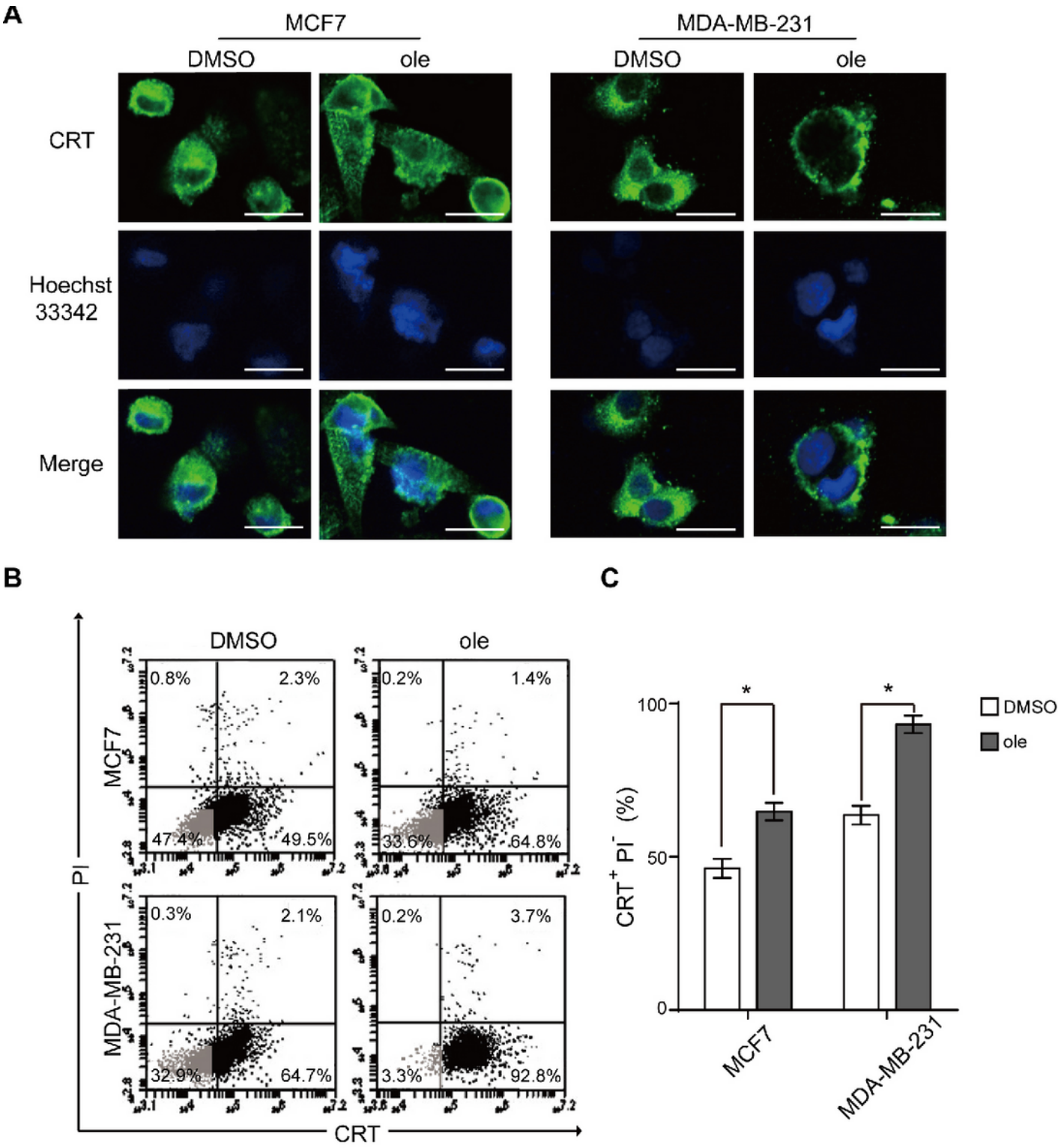

Figure 1

Oleandrin induces CRT exposure in breast cancer cells in vitro MCF7 and MDA-MB-231 cells were treated with oleandrin for 10 h. (A) Immunofluorescence analysis of cells stained with CRT and Hoechst 33342. Scale bar = 20 μm. (B) Cells were stained with CRT and PI and detected by flow cytometry. (C) The CRT-positive and PI-negative cells were showed in representative dot plots and quantification data. Data are

presented as means ± standard error of the mean from three independent experiments (*p <0.05). ole, oleandrin.

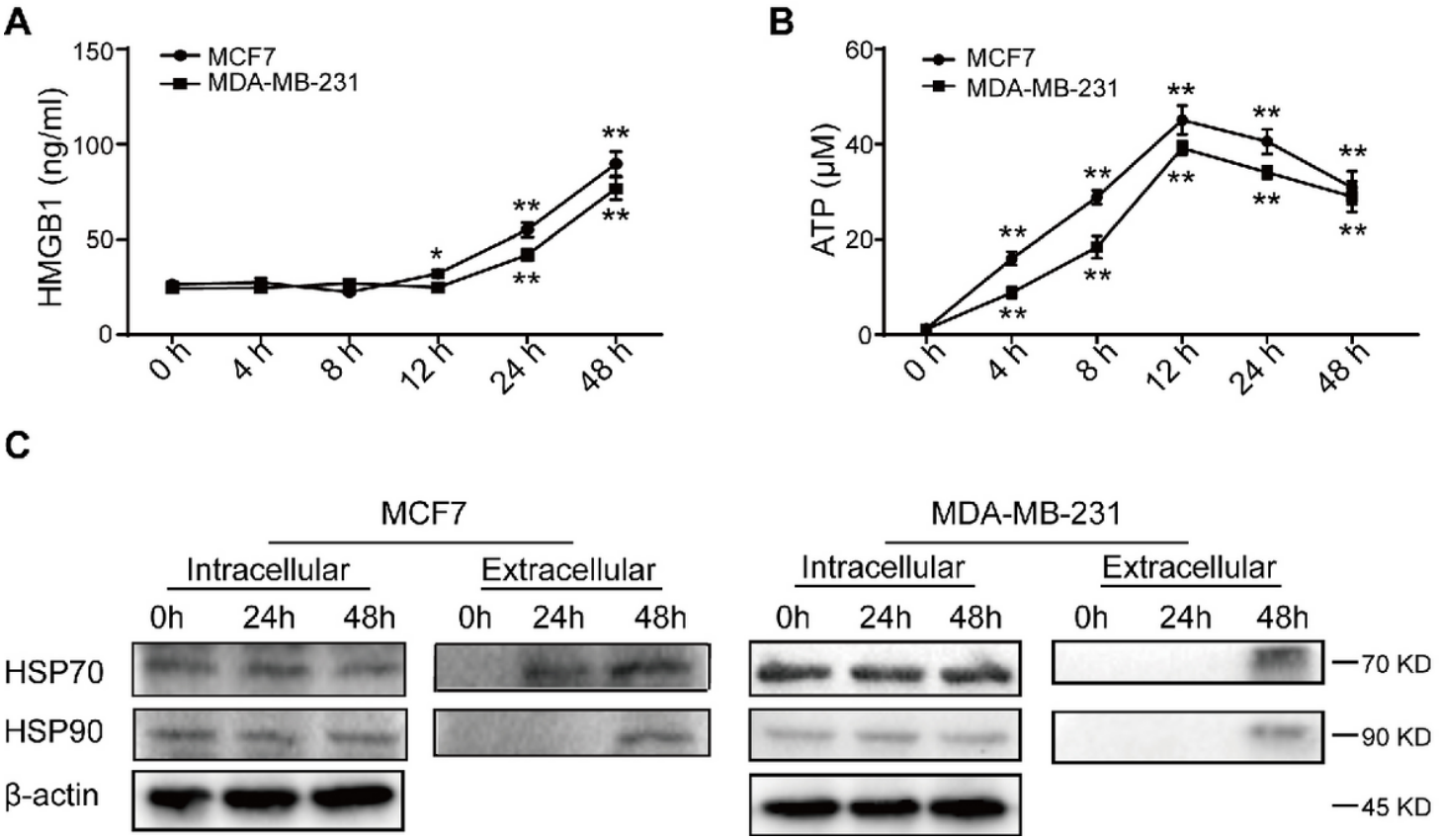

Figure 2

Oleandrin induces HMGB1 and ATP releasements. MCF7 and MDA-MB-231 cells were treated with oleandrin and culture supernatants were collected 4 h, 8 h, 12 h, 24 h and 48 h after treatment. (A) Secreted HMGB1 was detected by ELISA. (B) ATP secretion was detected by chemiluminescence assay. *p<0.05, **p<0.01 vs. untreated control cells. (C) Cell supernatants were collected and concentrated at 0 h, 24 h and 48 h after oleandrin treated. At the same time cell lysates were collected. The expression of HSP70 and HSP90 were detected by western blotting (WB).

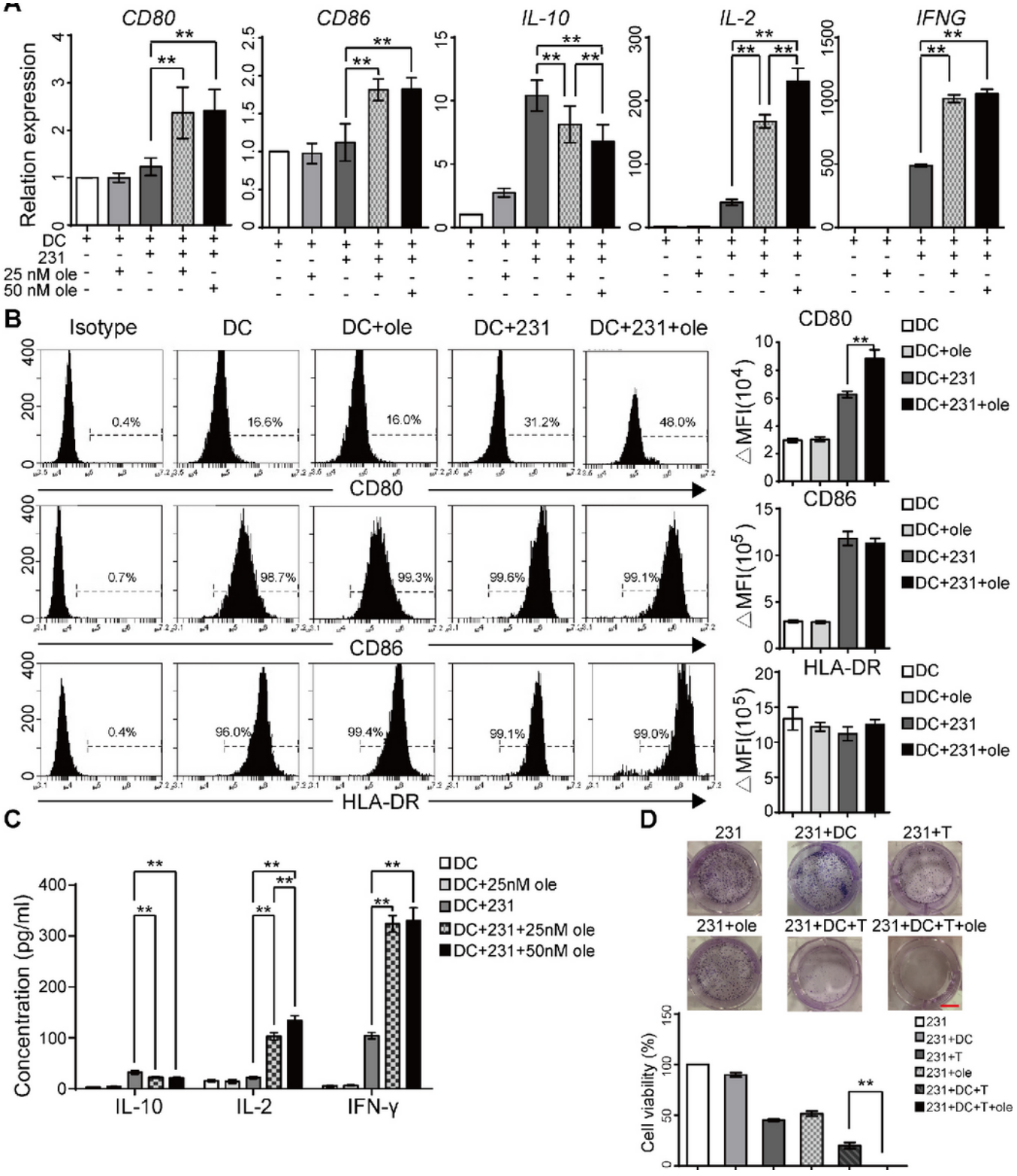

Figure 3

Oleandrin induces ICD associated immune activation in vitro DCs were co-cultured with MDA-MB-231 with or without oleandrin treatment for 48 h. DCs were sorted by staining with CD45. (A) The relative expression of CD80, CD86, IL-10, IL-2 and IFNG in DCs were detected by qRT-PCR. (B) The expression of CD80, CD86 and HLA-DR on DCs surface were further detected by flow cytometry. Cells stained with isotype antibody were used as control. Data were represented by ΔMFI values. (C) Cytokines expression

in the co-culture supernatants were further confirmed by ELISA. (F) The cell growth of the following groups was determined by clone formation assay: MDA-MB-231, MDA-MB-231/DCs, MDA-MB-231/CD8+ T cells, MDA-MB-231/DCs/CD8+ T cells, 25nM oleandrin-treated MDA-MB-231 and 25nM oleandrin-treated MDA-MB-231/DCs/CD8+ T cells. The representative pictures (upper) and quantification data (lower) were shown **p<0.01. 231, MDA-MB-231; ole, oleandrin.

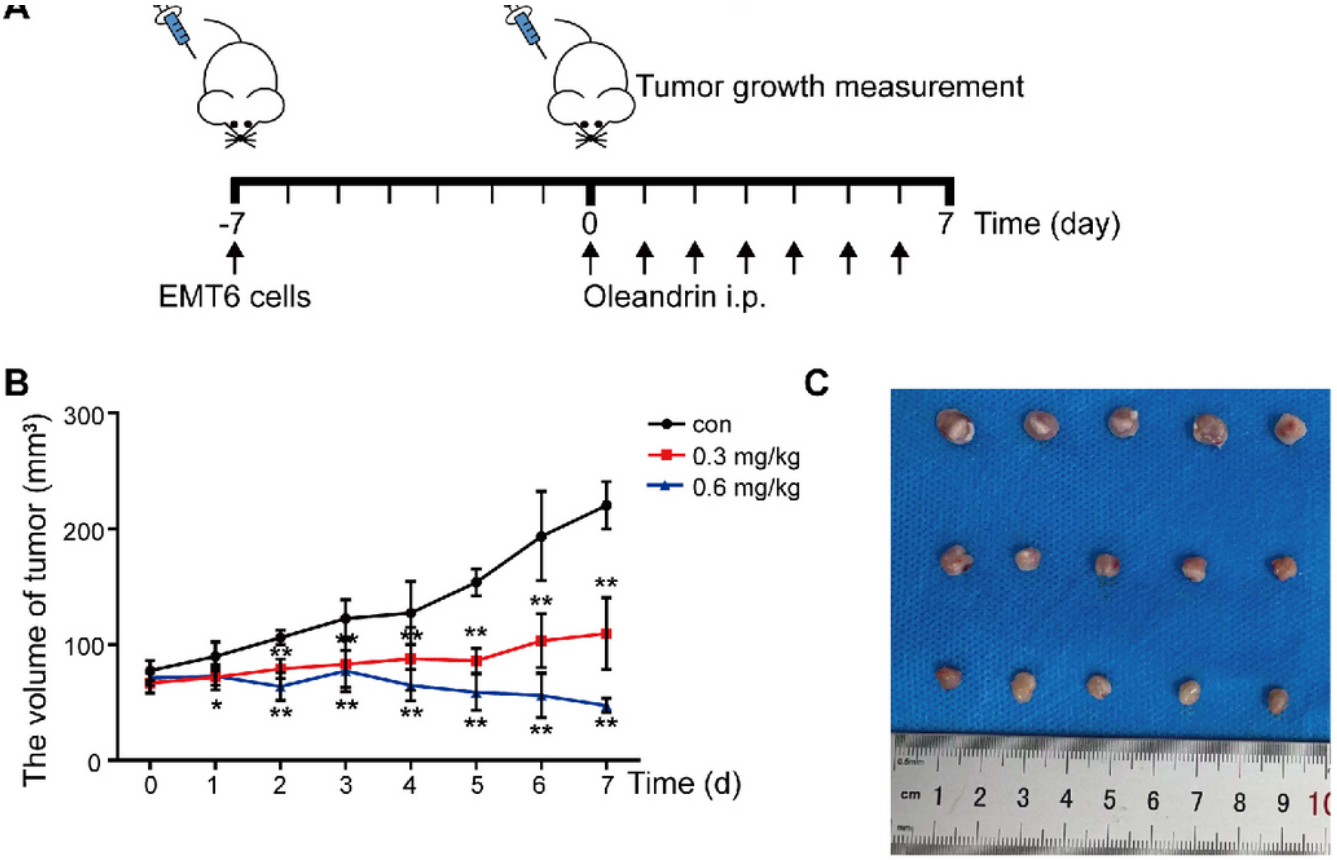

Figure 4

Oleandrin suppresses tumor growth in mice (A) Diagram of procedure for mouse tumor model. 2×105 EMT-6 cells were transplanted into mammary fat of BALB/c mice. 7 days after transplantation, tumor-bearing mice were divided into three groups and treated with oleandrin at 0.3mg/kg and 0.6mg/kg in peritoneal for 7 days. Mice treated with PBS were used as control. (B) Tumor volume was measured every day and quantified as 0.5 × length × width × width. The volume was expressed as the Mean ± SD (n = 5) and represented as tumor volume-time curves to show (*p<0.05, **p<0.01 vs. control.). (C) After 7-day administration, mice were sacrificed, and tumors were weighted. The representative tumors were shown. (D) Tumor weight in each group was expressed as the Mean ± SD (n = 5, **p < 0.01 vs. control.).

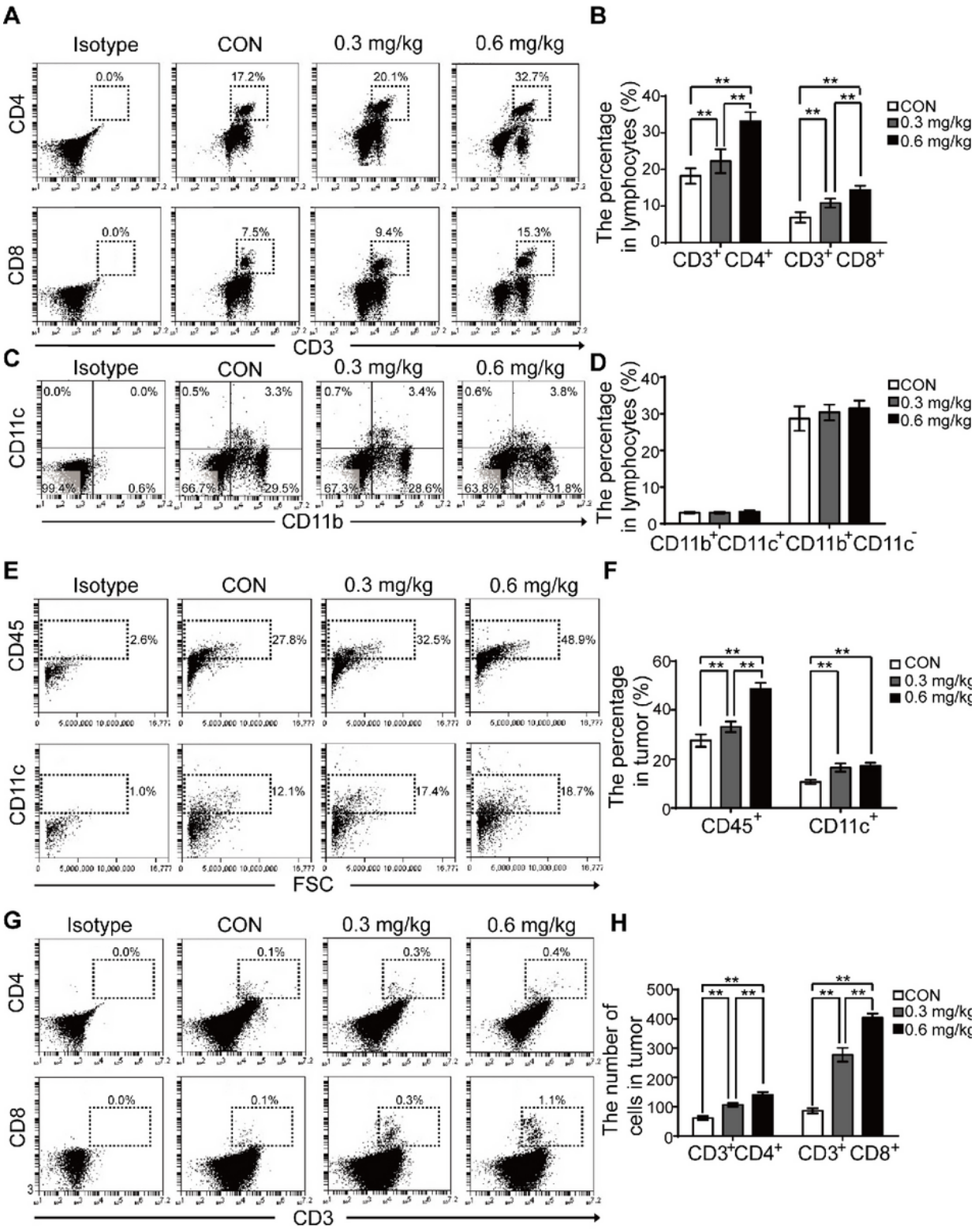

Figure 5

Oleandrin activates antitumor immune response in mice Splenocytes and tumor primary cells were collected from the tumor-bearing mice and detected by flow cytometry. (A-D) The frequency of T cells and DCs were analyzed by staining with CD4, CD8, CD3, CD11b and CD11c. The results were represented as percentage of gated lymphocytes. (E and F) Tumor infiltrating lymphocytes (TIL) and tumor infiltrating DCs were analyzed by staining with CD45 and CD11c. The results were represented as percentage in

tumors. (G and H) The absolute number of CD4+ and CD8+ T cell in tumors were expressed as the Mean ± SD. n = 5, **p < 0.01 vs. control. CON, control.

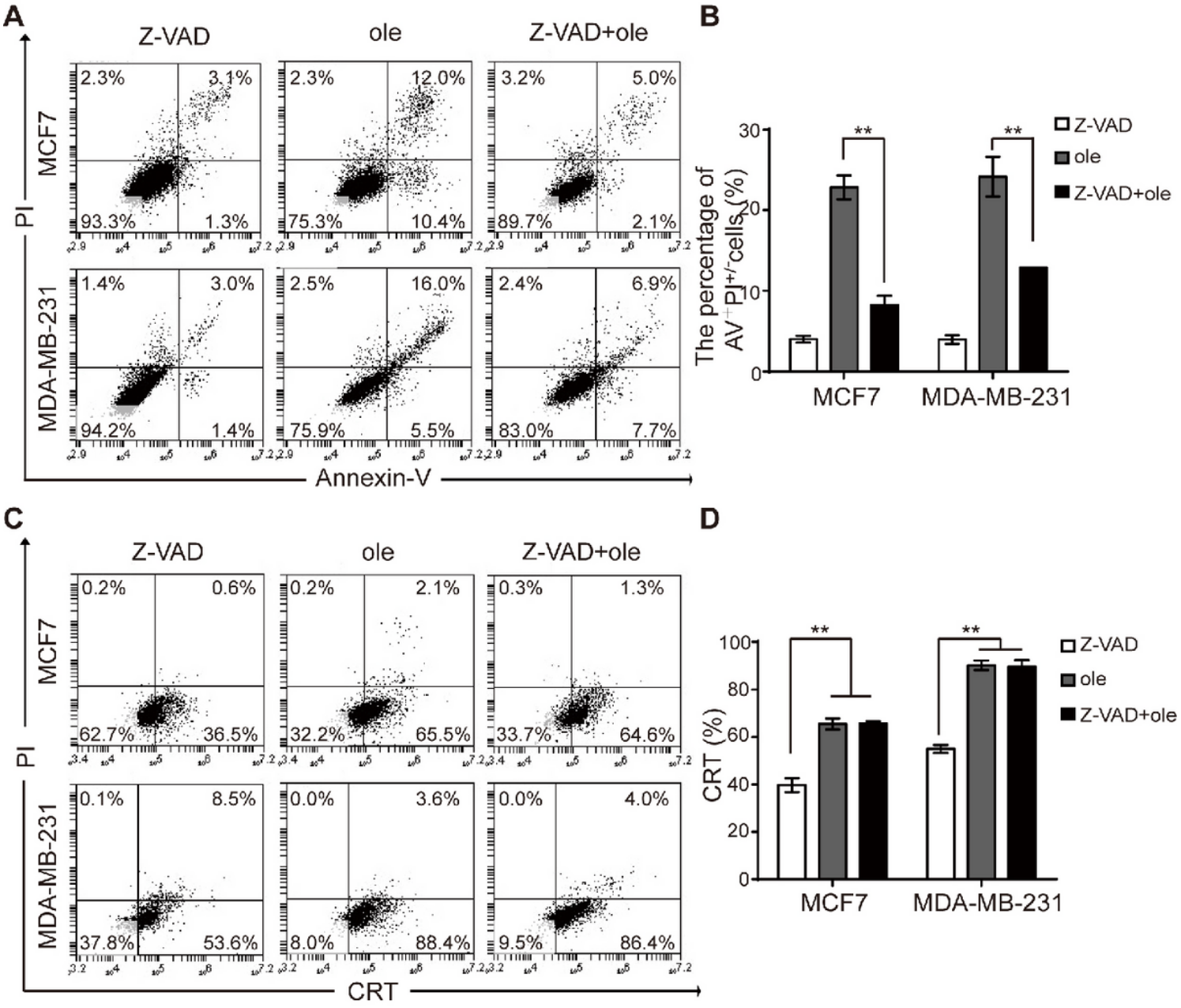

Figure 6

Oleandrin induces CRT exposure was independent with caspase activity. The MCF7 and MDA-MB-231 cells were pretreated with pan-caspase inhibitor Z-VAD-FMK for 10 h, then treated with oleandrin for further 24 h. (A) Cell apoptosis was detected by staining with Annexin-V and PI. (B) The apoptosis rate (Annexin-V+ and PI+/-) was shown as the Mean ± SD (n = 3, **p < 0.01 vs. control). (C) and (D) The CRT exposure on cell surface was detected by flow cytometry. The percentage of CRT+ and PI- cells were shown as the Mean ± SD (n = 3, **p < 0.01 vs. control). AV, Annexin-V; ole, oleandrin.

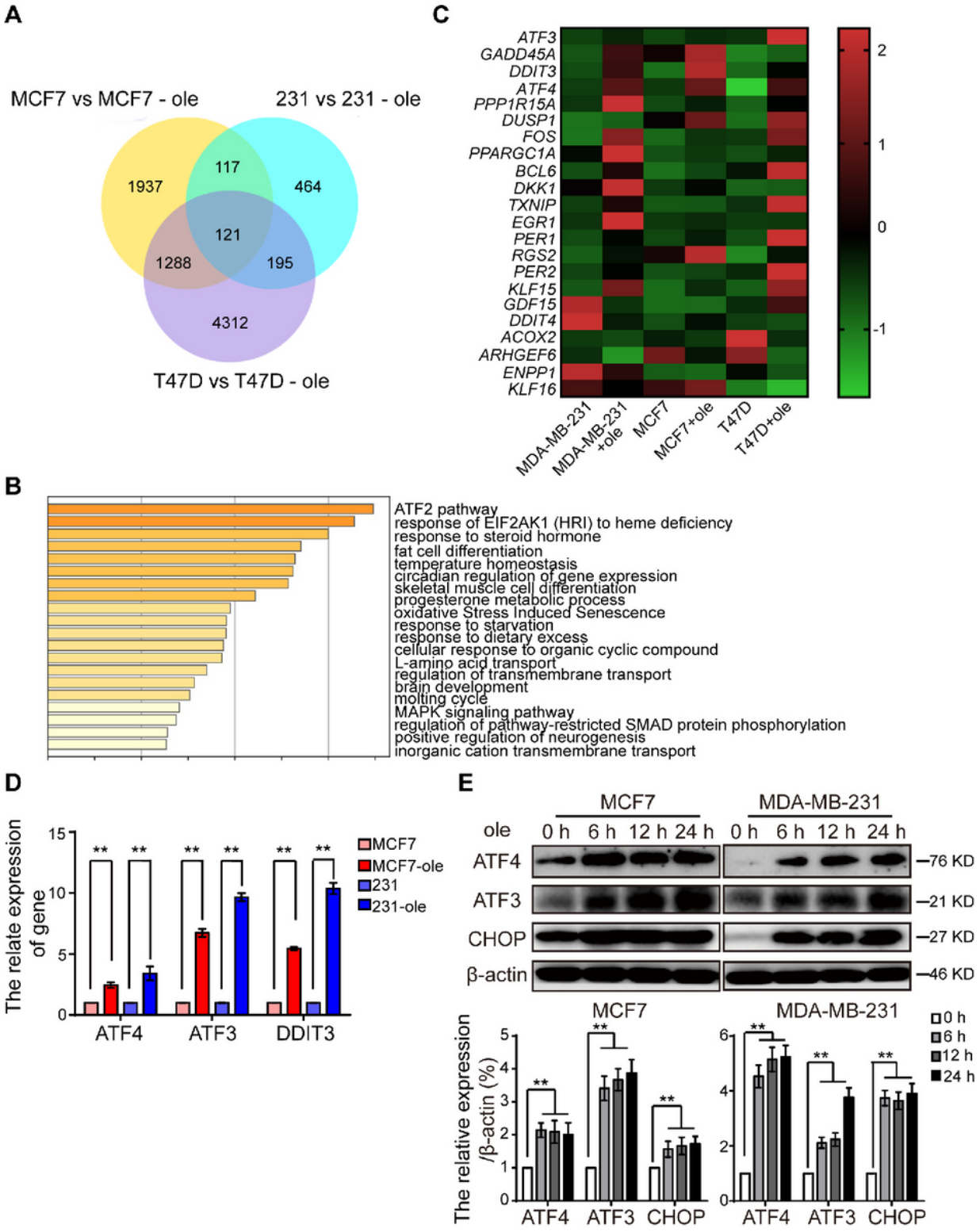

Figure 7

Oleandrin induces CRT exposure was independent with caspase activity. The MCF7 and MDA-MB-231 cells were pretreated with pan-caspase inhibitor Z-VAD-FMK for 10 h, then treated with oleandrin for further 24 h. (A) Cell apoptosis was detected by staining with Annexin-V and PI. (B) The apoptosis rate (Annexin-V+ and PI+/-) was shown as the Mean ± SD (n = 3, **p < 0.01 vs. control). (C) and (D) The CRT

exposure on cell surface was detected by flow cytometry. The percentage of CRT+ and PI- cells were shown as the Mean ± SD (n = 3, **p < 0.01 vs. control). AV, Annexin-V; ole, oleandrin.

Fig.8

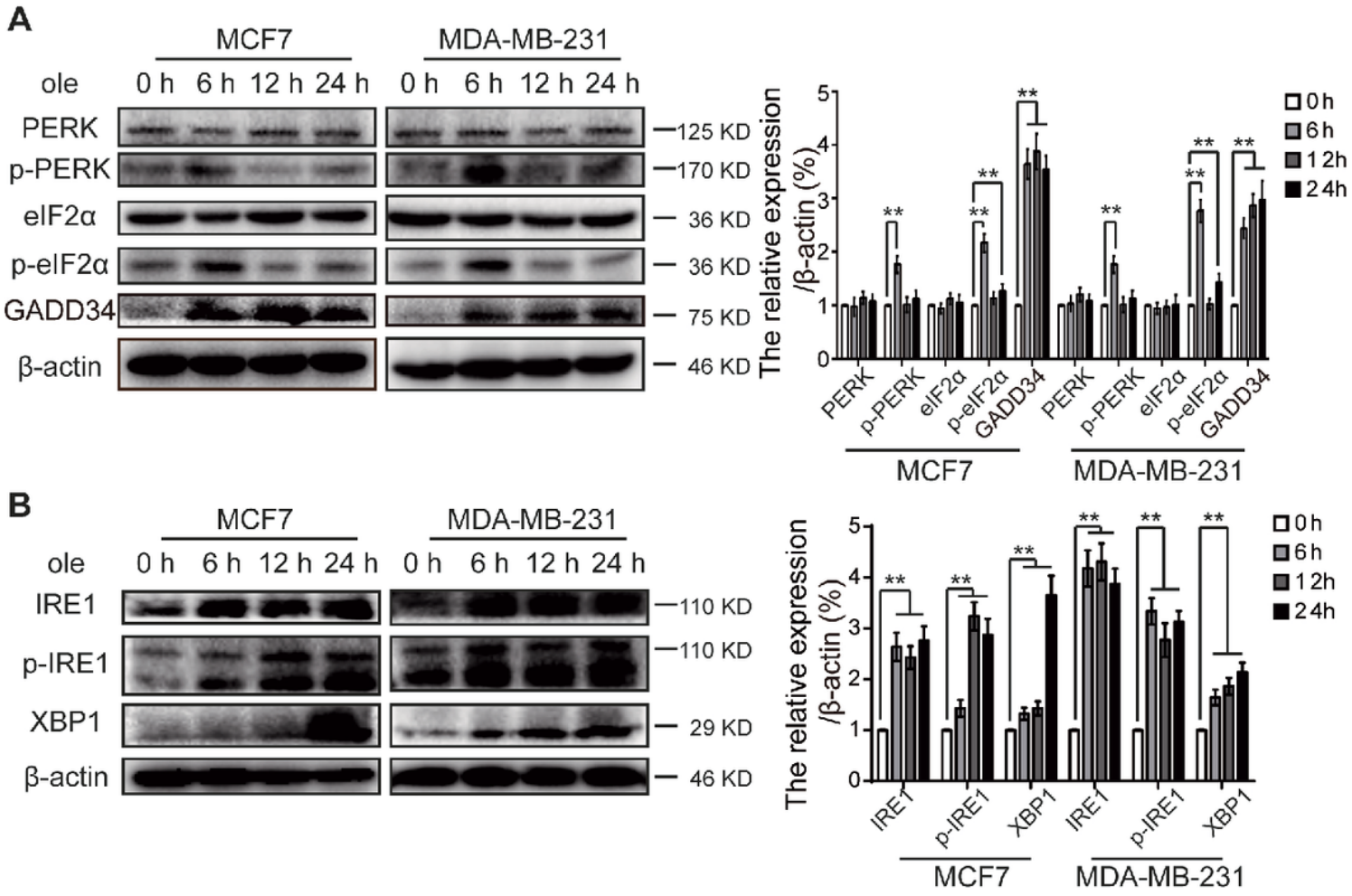

Figure 8

Oleandrin induces breast cancer ER stress (A) and (B) MCF7 and MDA-MB-231 cells were treated with oleandrin for 0 h, 6 h, 12 h and 24 h. The protein expressions were analyzed by western blotting. β-actin was used as loading control.

Fig.9

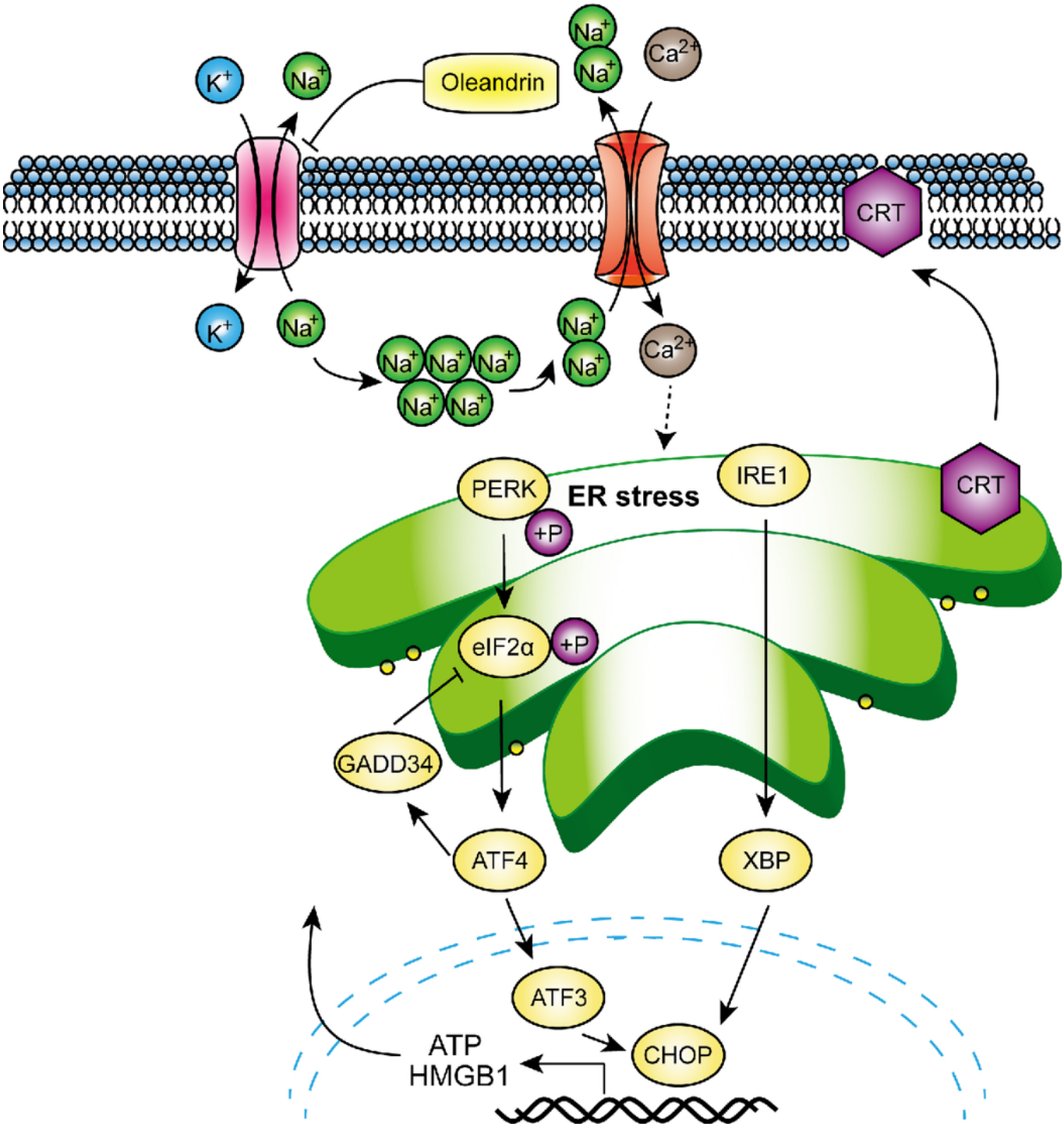

Figure 9

Proposed model of oleandrin induced ICD in breast cancer Oleandrin, as a Na+/K+ ATPase inhibitor, increases the concentration of Na+ and activated Na+/Ca2+ ion exchange channel on cell surface, which causes the influx of Ca2+. Loss of cellular homeostasis and disruption of Ca2+ leads to activation of ER stress associated pathways including PERK-eIF2α-ATF4 and IRE1-XBP1. ER stress enhances the

releasement of ATP and HMGB1. Moreover, ER stress induces CRT exposure to the cell surface. The release of these DAMPs signals eventually leads to the enhancement of immune response.

Supplementary Files

This is a list of supplementary files associated with this preprint. Click to download.

- sFig.pdf